JOURNAL OF AGRICULTURAL AND FOOD CHEMISTRY

Monitoring Biochemical Changes in Bacterial Spore during Thermal and Pressure-Assisted Thermal Processing using FT-IR Spectroscopy

ANAND SUBRAMANIAN, JUHEE AHN,† V. M. BALASUBRAMANIAM, AND LUIS RODRIGUEZ-SAONA*

Department of Food Science and Technology, Ohio State University, 2015 Fyffe Court, Columbus, Ohio 43210

Pressure-assisted thermal processing (PATP) is being widely investigated for processing low acid foods. However, its microbial safety has not been well established and the mechanism of inactivation of pathogens and spores is not well understood. Fourier transform infrared (FT-IR) spectroscopy was used to study some of the biochemical changes in bacterial spores occurring during PATP and thermal processing (TP). Spore suspensions ($\sim 10^9$ CFU/mL of water) of *Clostridium tyrobutyricum, Bacillus sphaericus,* and three strains of *Bacillus amyloliquefaciens* were treated by PATP (121 °C and 700 MPa) for 0, 10, 20, and 30 s and TP (121 °C) for 0, 10, 20, and 30 s. Treated and untreated spore suspensions were analyzed using FT-IR in the mid-infrared region (4000–800 cm^{-1}). Multivariate classification models based on soft independent modeling of class analogy (SIMCA) were developed using second derivative-transformed spectra. The spores could be differentiated up to the strain level due to differences in their biochemical composition, especially dipicolinic acid (DPA) and secondary structure of proteins. During PATP changes in α-helix and β-sheets of secondary protein were evident in the spectral regions 1655 and 1626 cm^{-1}, respectively. Infrared absorption bands from DPA (1281, 1378, 1440, and 1568 cm^{-1}) decreased significantly during the initial stages of PATP, indicating release of DPA. During TP changes were evident in the bands associated with secondary proteins. DPA bands showed little or no change during TP. A correlation was found between the spore's Ca-DPA content and its resistance to PATP. FT-IR spectroscopy could classify different strains of bacterial spores and determine some of the changes occurring during spore inactivation by PATP and TP. Furthermore, this technique shows great promise for rapid screening PATP-resistant bacterial spores.

KEYWORDS: Pressure-Assisted Thermal Processing; Infrared Spectroscopy; Spore Inactivation; Dipicolinic acid; Spore Resistance

INTRODUCTION

Generally bacterial spores have higher resistance to processing than vegetative cells. Inactivation of bacterial spores while retaining the nutritional and organoleptic qualities of food is a challenge to the food industry. Due to the adverse effect of traditional thermal processing on the nutritional quality of food products alternative food processing methods such as high pressure processing are being developed (*1*). Despite its advantages, high pressure processing at room temperature may be ineffective in inactivating spores and combined pressure and temperature processing has been suggested as an alternative (*1*, *2*).

Pressure-assisted thermal processing (PATP) involves combined application of pressure and temperature to process foods. The pressure and temperature may range from 600 to 900 MPa and from 90 to 121 °C, respectively (*3*, *4*). Pressure-assisted thermal processing, with its advantages such as rapid and uniform heating and reduced thermal damage, offers many opportunities to develop food products with microbiological stability, longer shelf-life, and better nutritional and organoleptic quality. Processing of low-acid food products such as eggs, soups, tea, coffee, and potatoes is a widely researched application of PATP. Many researchers have investigated the application of combined pressure and temperature processing to inactivate bacterial spores (*4*–*9*). However, like many other sterilization processing methods, the exact mechanism of inactivation of bacterial spores during PATP is not well understood. In advancing the applications of PATP it is essential to understand the effect of processing parameters on the destruction of spores.

Many factors including sporulation temperature, type of treatment, spore water content, dipicolinic acid (DPA) level,

* To whom correspondence should be addressed. Phone: 614-292-3339; fax: 614-292-0218; e-mail: rodriguez-saona.1@osu.edu.

† Current Address: Division of Biomaterials Engineering, School of Bioscience and Biotechnology, Kangwon National University, Chuncheon 200–701, South Korea.

10.1021/jf0708241 CCC: $37.00
Published on Web 10/02/2007

small acid-soluble proteins, minerals, etc. influence the thermal inactivation mechanism of bacterial spores. These factors have been researched and reviewed in detail by many (*10–14*), although their precise role is unknown. The role of DPA, which constitutes around 10% of the spore's dry weight (*14*), in spore resistance, is a topic that has provoked considerable discussion. While it has been fairly well established that DPA plays no role in spore resistance to dry heat (*15*), its role in spore wet-heat resistance is still unclear. Although some correlation has been reported between DPA and spore wet heat resistance, some DPA-less spores still retained their wet heat resistance (*14*). Some researchers have concluded that resistance to combined pressure and temperature treatments depend on their ability to retain DPA (*6, 7*). Many studies have investigated the correlation between spore composition, especially DPA content and resistance to pressure and heat (*7, 15–17*). Almost all of these studies employ time-consuming traditional plating techniques, extraction methods, or chromatographic techniques. The typical longer incubation periods required for spores further increase the analysis time. Fourier transform infrared (FT-IR) spectroscopy offers a unique possibility of rapidly monitoring spore inactivation and related biochemical changes in composition of spores including DPA with minimum sample preparation.

FT-IR spectroscopy produces specific spectral patterns based on the chemical composition of the sample, which enables strain-level discrimination and identification. Numerous studies over the past few decades have used FT-IR to characterize bacteria (*18*). More recently, several studies have attempted to extend this technique to monitor bacterial spores and their composition (*19–24*). Our group has demonstrated the potential of FT-IR spectroscopy combined with regression multivariate analysis to predict viable spore concentrations in samples treated by PATP and thermal processing (TP), based on differences in biochemical composition (*19*). This research paper expands from our previous work by evaluating the collected FT-IR spectral information using classification pattern recognition analysis to further our understanding of the biochemical changes occurring in bacterial spores during PATP and TP. Understanding spore inactivation mechanisms during PATP will help in optimizing process parameters, and attaining food safety goals.

MATERIALS AND METHODS

Bacterial Spore Production and Thermal and Pressure-Assisted Thermal Processing of Spores. *Bacillus amyloliquefaciens* TMW 2.479 Fad 82 and *B. amyloliquefaciens* TMW 2.482 Fad 11/2 were provided by M. Gänzle, Lehrstuhl für Technische Mikrobiologie, Technische Universität München (Freising, Germany). *Bacillus amyloliquefaciens* ATCC 49764 and *C. tyrobutyricum* ATCC 25755 were purchased from American type Culture Collection (Manassas, VA). *Bacillus sphaericus* NZ 14 was provided by R. Robertson, Fonterra Research Centre (Palmerston North, New Zealand). The conditions for bacterial cultivation were previously described by Ahn and collaborators (*5*). Briefly, *B. amyloliquefaciens* and *B. sphaericus* strains were cultivated aerobically in trypticase soy broth supplemented with 0.1% yeast extract (Difco, Detroit, MI) for 24 h at 32 and 37 °C, respectively. *Clostridium tyrobutyricum* was cultivated anaerobically in reinforced clostridial medium (Oxoid Inc., Ogdensburg, NY) and incubated at 37 °C for 24 h. Spores were produced as described by Ahn et al. (*5*). The cultures were spread plated and incubated up to 15 days until 95% sporulation was observed by microscopic examination. The spores were harvested in deionized water, sonicated, heat-shocked, and centrifuged. The spore pellets were resuspended in deionized water ($\sim 10^9$ spores/mL) and stored at 4 °C prior to PATP and TP within 30 days of preparation.

TP and PATP of spores were performed as described Ahn et al. (*5*) and Subramanian et al. (*19*). Thermal inactivation of *B. amyloliquefaciens* TMW 2.479 Fad 82 and TMW 2.482 Fad 11/2 spores was carried out at 121 °C. The come-up-time (time to attain the set process conditions) was approximately 3.0 min. Spore suspensions were treated for 0 (come-up-time), 10, 20, and 30 s holding times. Pressure-assisted thermal processing of spore samples was carried out using custom-fabricated high pressure kinetic testing equipment (PT-1, Avure Technologies, Kent, WA). Spore suspensions were processed at a temperature of 121 °C and 700 MPa for 0 (come-up-time), 10, 20, and 30 s. The come-up-time of the equipment was 30 s. Freshly harvested untreated spore suspension was used as a control. Total viable spores in TP and PATP treated samples was determined by the pour plating method according to the U.S. FDA Bacteriological Analytical Manual (BAM) procedure and has been reported previously (*5*).

Fourier Transform Infrared Spectroscopy and Multivariate Analyses. FT-IR spectroscopy of the spore samples was carried as described by Subramanian et al. (*19*), on an Excalibur 3500GX FT-IR spectrometer (Digilab, Randolph, MA). Aliquots (200 μL) of the samples were washed with distilled water, centrifuged, and resuspended in water. Exactly 10 μL was placed on the attenuated total reflectance (ATR) accessory with an AMTIR crystal (Pike Technologies, Madison, WI), vacuum dried, and scanned in the mid-infrared region (4000 and 800 cm^{-1}). For each of the two independently produced and treated spore samples between three and five spectra were collected, resulting in 6–10 spectra per sample per treatment time.

Multivariate analyses of the data were carried out using a chemometrics modeling software called Pirouette (v3.11, Infometrix Inc., Woodville, WA). For analysis, spectra were imported into Pirouette, mean-centered, transformed into their second derivative using a Savitzky-Golay polynomial filter (five-point window), and vector-length normalized. Discrimination of the spores was carried out using classification analysis based on soft independent modeling of class analogy (SIMCA). The data were projected onto principal component axes to visualize clustering of the five different strains of spores analyzed. The discriminating power plots provided by SIMCA were used to identify the infrared bands that were responsible for differentiating the five strains and to determine the biochemical changes in the spore composition during PATP and TP.

RESULTS AND DISCUSSION

Pattern recognition analysis of infrared spectral data acquired during inactivation of *Bacillus amyloliquefaciens* Fad 82, *B. amyloliquefaciens* Fad 11/2, *B. amyloliquefaciens* ATCC 49764, *B. sphaericus* NZ 14, and *Clostridium tyrobutyricum* ATCC 25755 by PATP and TP (*19*) was used to obtain some insight on structural and biochemical changes in spores occurring during processing. Drying spore suspension on the ATR crystal resulted in the formation of a uniform film of sample allowing for the collection of high-quality spectra with distinct spectral features that were very consistent within each sample. The raw spectra were transformed into their second derivatives for analyses to remove the baseline shifts, improve the peak resolution, and reduce the variability between replicates (*25*). The raw spectra and the transformed spectra of *Bacillus amyloliquefaciens* Fad 82 are shown in **Figure 1**. FT-IR spectra reflect the total biochemical composition of the bacterial spore, with bands due to major cellular constituents such as water, lipids, polysaccharides, acids, etc. The region from 4000 to 3100 cm^{-1} consists of absorbance from O–H and N–H stretching vibrations of hydroxyl groups and Amide A of proteins, respectively. Protein bands also appear in the regions 1700–1550 cm^{-1} (amide I and amide II) and 1310–1250 cm^{-1} (amide III). The C–H stretching vibrations of CH_3 and $>CH_2$ functional groups appear between 3100 and 2800 cm^{-1}. The spectral range 1250–800 cm^{-1} consists of signals from phosphodiesters and carbohydrates. The region between 1800 and 1200 cm^{-1} has been reported to contain almost all signals of interest in studying spore inactivation during PATP and TP (*19*).

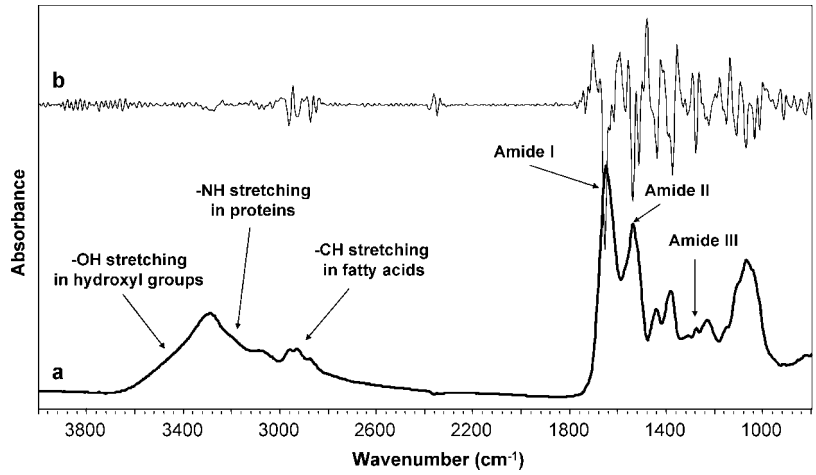

Figure 1. Raw and derivatized spectra of *Bacillus amyloliquefaciens* Fad 82 spore prepared in distilled water and measured on a three-bounce AMTIR-ATR crystal. (**a**) Fourier transform mid-infrared spectra of *B. amyloliquefaciens* Fad 82 spores obtained in the region 4000–800 cm^{-1} (**b**) Transformed (Savitzky-Golay 2nd derivative, five-point window) mid-infrared spectra of *B. amyloliquefaciens* Fad 82 spores.

Classification of Bacterial Spores. Classification models based on soft independent modeling of class analogy (SIMCA) were developed using the transformed spectra of *Bacillus amyloliquefaciens* Fad 82, *B. amyloliquefaciens* Fad 11/2, *B. amyloliquefaciens* ATCC 29764, *B. sphaericus* NZ 14, and *Clostridium tyrobutyricum* ATCC 25755. SIMCA is a principal component analysis method that creates a 3D model incorporating all the classes (different samples) by computing a small number of orthogonal variables (principal components or PCs). The samples are projected on to top three PCs which explain as much of the variation as possible between all the samples in that class, preserving relevant information and reducing noise (*26*). The SIMCA class projection plot (**Figure 2**) allowed for visualization of the sample clusters on the three PC axes and showed that all the five strains formed distinct clusters that were well separated in 3D space. *Bacillus amyloliquefaciens* Fad 82 and *B. amyloliquefaciens* Fad 11/2 (clusters 4 and 5) clustered far from other strains and very close to each other, indicating their very similar chemical composition. This reaffirms the capability of FT-IR combined with multivariate analysis for classifying and identifying spores up to the strain level based on biochemical differences.

The spectral wavenumbers and the associated functional groups that were responsible for the classification of the spores in SIMCA class projections can be identified using the discriminating power plot. In the discriminating power plot each wavenumber in the spectral range is plotted against its power in discriminating the samples that are being compared. The higher the value of discriminating power, the greater is the influence of that wavenumber in classifying the samples. The discriminating power plot and the important spectral wavenumbers responsible for the classification of the five strains of bacterial spores are shown in **Figure 3A**. The discriminating power was relatively high (~7000 units), indicating that the composition of the strains were significantly different. The FT-IR spectra of various bacterial spore functional groups, including DPA and Ca-DPA, and their corresponding band assignments have been published earlier (*19, 20, 23*). The major discriminating band was 1626 cm^{-1}, which corresponds to amide I band of β-pleated sheets of secondary proteins. The bands associated with Ca-DPA (1281, 1378, 1440, and 1616 cm^{-1}) greatly influenced the classification. Bands of DPA (1568, and 1695 cm^{-1}) also contributed to the classification, although not to the extent as Ca-DPA. Amide I band of α-helical structure of

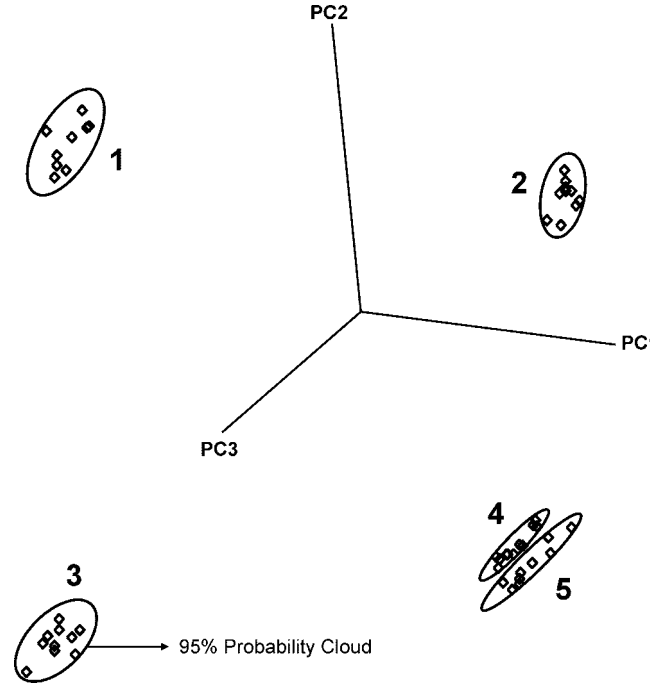

Figure 2. Soft independent modeling of class analogy class projections of *Bacilli* and *Clostridia* spores. 1) *Bacillus sphaericus* NZ 14, 2) *B. amyloliquefaciens* ATCC 49764, 3) *Clostridium tyrobutyricum* ATCC 25755, 4) *B. amyloliquefaciens* Fad 82, and 5) *B. amyloliquefaciens* Fad 11/2. The mid-infrared spectra were transformed (Savitzky-Golay second derivative, five-point window) and vector-length-normalized before analysis.

secondary proteins at 1655 cm^{-1} was another protein band discriminating the classes.

The most different strains in the classification model, in terms of composition, were *B. amyloliquefaciens* Fad 82 and *C. tyrobutyricum* ATCC 25755. These two strains were previously identified as the most and the least resistant strains to PATP and TP (*5, 6, 19*). The main compositional differences between these two strains are highlighted in **Figure 3B**. The discriminating power was relatively very high (~30000 units), indicating that the two strains were extremely different in composition. The spectral bands corresponding to DPA and Ca-DPA (1281, 1378, 1568, and 1695 cm^{-1}) and secondary proteins (1626 and 1655 cm^{-1}) contributed to the differentiating *B. amyloliquefaciens* Fad 82 from *C. tyrobutyricum*. This indicates that the DPA

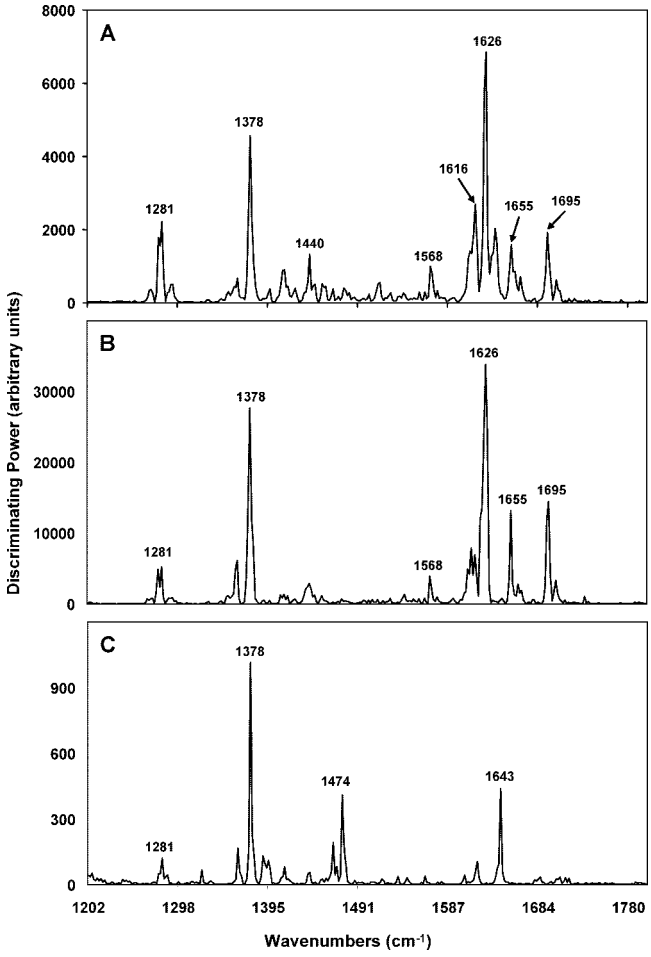

Figure 3. Discriminating power in classification of bacterial spores. Prominent bands and their relative importance in discriminating (**A**) all five spores investigated in this study, (**B**) *Bacillus amyloliquefaciens* Fad 82 from *Clostridium tyrobutyricum* ATCC 25755, and (**C**) *B. amyloliquefaciens* Fad 82 from *B. amyloliquefaciens* Fad 11/2. Spectral bands that influence the classification are highlighted.

and secondary protein content are very different among these strains and may possibly be related to their differences in PATP- or TP-resistance. The discriminating power between the two very closely related strains *B. amyloliquefaciens* Fad 82 and *B. amyloliquefaciens* Fad 11/2 was relatively very low (~950 units); with the major differentiation due to Ca-DPA chelate (**Figure 3C**). Comparison of the normalized-spectra of the two strains showed that the absorption from Ca-DPA chelate at 1378 cm^{-1} was slightly lower for *B. amyloliquefaciens* Fad 11/2 than *B. amyloliquefaciens* Fad 82 (data not shown). These two strains have earlier been reported to have high resistance to PATP and TP, with the resistance of *B. amyloliquefaciens* Fad 82 slightly higher than *B. amyloliquefaciens* Fad 11/2 (*5, 7, 19*). This minor difference in their resistance can be related to the small difference in Ca-DPA levels. The DPA in the spore core is most likely chelated with divalent cations, mainly Ca^{2+} (*14*). The Ca-DPA chelate is believed to play a role in dehydrating the spore core and there by increasing the wet heat resistance of spores (*10*). Two other bands, 1474 and 1643 cm^{-1}, were found to be different between *B. amyloliquefaciens* Fad 82 and *B. amyloliquefaciens* Fad 11/2 and can be attributed to amide II and amide I bands of proteins.

Biochemical Changes in Spores during Pressure-Assisted Thermal Processing. The spore suspensions were treated for 0, 10, 20, and 30 s holding times. The average number of survivors at each holding time during processing is summarized in **Table 1**. Comparison of the derivatized spectrum of PATP-treated spore with that of the untreated spore showed various differences in the regions corresponding to DPA and secondary proteins (**Figure 4**). The differences between samples can be better understood using a discriminating power plot that shows the relative contribution of each wavenumber in differentiating the samples. The differences in composition between control (untreated) and 0 s, 0 s and 10 s, 10 s and 20 s, and 20 s and 30 s PATP-treated *B. amyloliquefaciens* Fad 82 samples are shown in **Figure 5**. This plot essentially provides information on the changes in biochemical composition at every stage of PATP. A higher discriminating power value in this plot implies greater amount of change. Based on the discriminating power at every processing stage, it was found that most changes occurred during the come-up-time (line **a**, before the set temperature and pressure were attained) as compared to 0–10 s (line b), 10–20 s (line **c**), and 20–30 s (line **d**) of holding.

Peaks corresponding to DPA and secondary proteins showed significant changes during PATP treatment. The absorbance signal from Ca-DPA (1281, 1378, and 1440 cm^{-1}) and DPA (1568 cm^{-1}) reduced tremendously during come-up-time. This complete loss of signal from DPA-related bands indicates release of almost all DPA compounds from the spores. **Table 1** shows that inactivation of spores, except *C. tyrobutyricum* ATCC 25755, occurred gradually over a period that extended beyond the come-up-time. Therefore, complete release of DPA during come-up-time may not imply complete inactivation of spores, and this process may actually happen concurrently or after the release of DPA. All the strains exhibited similar trends. Margosch et al. (*7*) reported that DPA-free spores from pressure treatment lost their heat resistance. The authors also found that after more than 90% of the DPA was lost, high-pressure was not found to further influence spore inactivation and that further inactivation of the sensitized spores is caused by heat.

Comparison of Changes in Spores during Thermal and Pressure-Assisted Thermal Processing. Both PATP and TP caused rapid changes in the spores, almost all of which occurred during the come-up-time. The type and extent of changes that occurred in *B. amyloliquefaciens* Fad 82 and Fad 11/2 during come-up-time of PATP and TP are highlighted in **Figure 6**. The major changes that occurred in *B. amyloliquefaciens* Fad 82 during come-up-time of PATP are highlighted in **Figure 6**, line **a**. Interestingly, almost all of the changes evident in the spectra were related to Ca-DPA (1281, 1378, and 1440 cm^{-1}) and DPA (1568 cm^{-1}), which may be induced by pressure (*16, 17, 27, 29*). *Bacillus amyloliquefaciens* Fad 11/2 also had very similar changes during inactivation by PATP (**Figure 6**, line **b**) as well as those observed with *B. amyloliquefaciens* ATCC 49764 and *B. sphaericus* NZ 14, with minor variations in the relative amount of changes in each band (data not shown). *Clostridium tyrobutyricum* ATCC 25755, which has earlier been reported to be very sensitive to PATP and TP (*5, 19*), showed slightly different changes during PATP. Very subtle changes (low discriminating power values) were found to occur at 1655 (amide I bands of α-helical structure of secondary proteins), 1378 (COO^{-} group of Ca-DPA chelate) and 1281 (DPA band) cm^{-1} during PATP. Lower discriminating power at wavenumbers corresponding to DPA could be interpreted as low DPA content (especially Ca-DPA) in the spores of *C. tyrobutyricum*, which could adversely affect its wet heat resistance.

Similar to PATP, the derivatized spectra of untreated and TP-treated spores of *B. amyloliquefaciens* Fad 82 showed significant differences (**Figure 4**). Major changes were found in the bands

Table 1. Average Number of Survivors During Thermal and Pressure-Assisted Thermal Processing Determined by Plate Count Method[a]

	survivor population (Log CFU/ml)						
	Bacillus amyloliquefaciens Fad 82		*Bacillus amyloliquefaciens* Fad 11/2		*Bacillus amyloliquefaciens* ATCC 49764	*Bacillus sphaericus* NZ 14	*Clostridium tyrobutyricum* ATCC 25755
holding time (s)	PATP[b]	TP[c]	PATP[b]	TP[c]	PATP[b]	PATP[b]	PATP[b]
control	8.8 ± 0.1^{d}	9.1 ± 0.2^{d}	8.8 ± 0.2^{d}	8.4 ± 0.2^{d}	8.2 ± 0.1^{d}	8.4 ± 0.1^{d}	7.9 ± 0.2^{d}
0	3.9 ± 0.2^{e}	5.9 ± 0.0^{e}	3.4 ± 0.1^{e}	4.5 ± 0.0^{e}	3.0 ± 0.2^{e}	0.3 ± 0.1^{e}	UD
10	1.4 ± 0.0^{f}	4.1 ± 0.0^{f}	1.3 ± 0.1^{f}	2.2 ± 0.1^{f}	1.4 ± 0.0^{f}	0.3 ± 0.1^{e}	UD
20	1.4 ± 0.1^{f}	3.2 ± 0.1^{g}	0.9 ± 0.0^{h}	0.7 ± 0.1^{g}	1.0 ± 0.0^{g}	UD	UD
30	0.3 ± 0.0^{g}	1.7 ± 0.1^{h}	1.9 ± 0.2^{g}	UD	UD	UD	UD

[a] UD, Undetectable by plating method at a detection limit of 2 CFU/ml. [b] Pressure-assisted thermal processing (PATP) of the spore samples was carried out for 0, 10, 20 and 30 s at 121 °C and 700 MPa, after the initial come-up-time of 30 s. [c] Thermal processing (TP) of the spore samples was carried out for 0, 10, 20 and 30 s at 121 °C, after the initial come-up-time of 3 min. [d–h] Means (±standard deviation) with different subscript within a column are significantly different ($p < 0.05$).

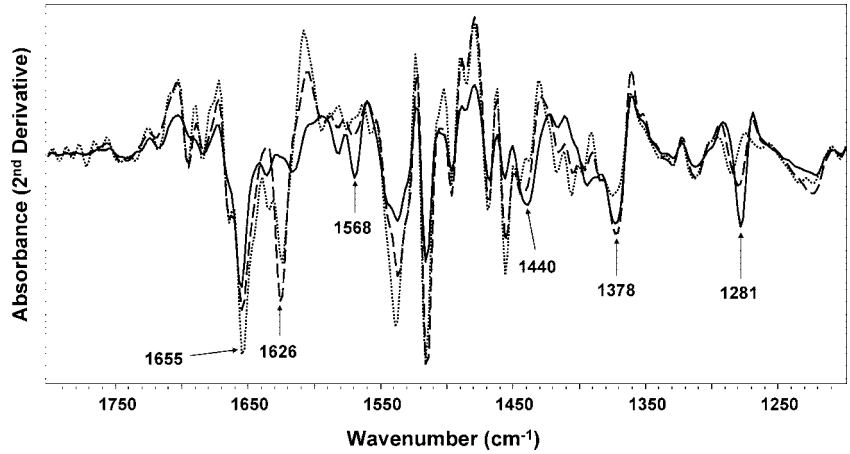

Figure 4. Changes in composition of *Bacillus amyloliquefaciens* Fad 82 during thermal and pressure-assisted thermal processing. The region 1800–1200 cm^{-1} was used in the analyses as almost all the changes were in this region. Derivatized (Savitzky-Golay 2nd derivative) spectra of (—) untreated *B. amyloliquefaciens* Fad 82, (- - -) *B. amyloliquefaciens* Fad 82 at the end of come-up-time during thermal processing, and (.....) *B. amyloliquefaciens* Fad 82 at the end of come-up-time during pressure-assisted thermal processing.

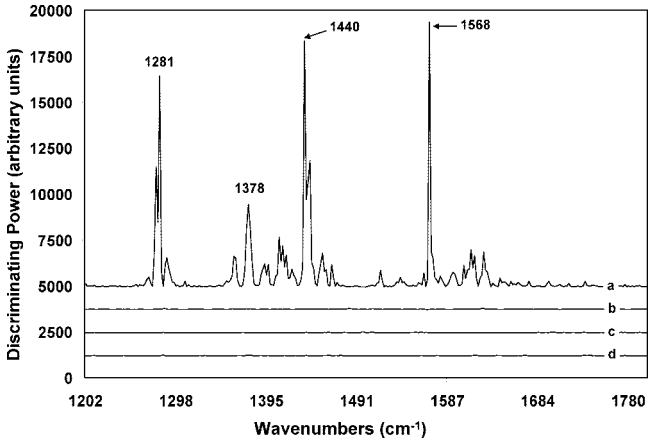

Figure 5. Discriminating powers in differentiating *Bacillus amyloliquefaciens* Fad 82 treated by pressure-assisted thermal processing for different holding times. Changes that occurred in *B. amyloliquefaciens* Fad 82, (**a**), during come-up-time, (**b**) from come-up-time to 10 s of holding, (**c**) from 10 to 20 s of holding, and (**d**) from 20 to 30 s of holding are highlighted. Higher the discriminating power value, the greater is the change.

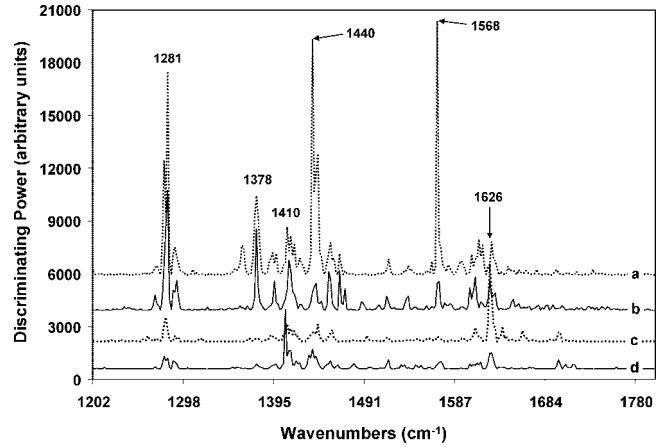

Figure 6. Biochemical changes in spore composition during come-up-time in (**a**) *Bacillus amyloliquefaciens* Fad 82 during PATP, (**b**) *B. myloliquefaciens* Fad 11/2 during PATP, (**c**) *B. amyloliquefaciens* Fad 82 during TP, and (**d**) *B. amyloliquefaciens* Fad 11/2 during TP. The come-up-time for PATP and TP was 30 s and 3 min, respectively.

associated with secondary proteins. The DPA bands showed little or no changes. Almost all changes in the spore composition occurred during the come-up-time. **Figure 6** (lines **c** and **d**) show the changes that occurred in the composition of *B. amyloliquefaciens* Fad 82 and *B. amyloliquefaciens* Fad 11/2 during come-up-time of TP. The two *B. amyloliquefaciens* strains exhibited slightly different changes during the come-up-time of TP. The major change in *B. amyloliquefaciens* Fad 82 was found to occur in the region 1626 cm^{-1}, which is associated with amide I bands of β-pleated sheets of secondary proteins (**Figure 6**, line **c**). Minor changes were also observed 1281 and 1410 cm^{-1}, which correspond to DPA and C–O–H bending of lipids, carbohydrates, and proteins, respectively. Unlike *B. amyloliquefaciens* Fad 82, *B. amyloliquefaciens* Fad

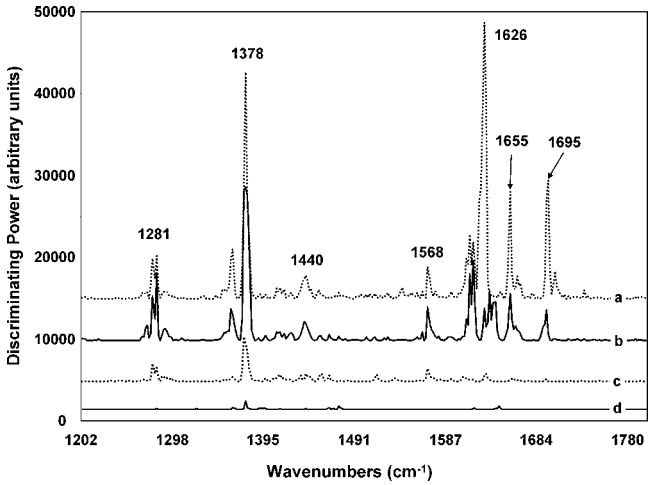

Figure 7. Differences in the biochemical composition of *Bacillus amyloliquefaciens* Fad 82 and (**a**) *Clostridium tyrobutyricum* ATCC 25755, (**b**) *B. sphaericus* NZ 14, (**c**) *B. amyloliquefaciens* ATCC 49764, and (**d**) *B. amyloliquefaciens* Fad 11/2. Greater the discriminating power value at a particular wavenumber the greater is difference in the functional groups associated with that wavenumber.

11/2 (**Figure 6**, line **d**) exhibited major changes at 1410 cm^{-1}, during both PATP and TP, and only minor changes at 1626 cm^{-1}.

Most of the changes during PATP were associated with DPA and Ca-DPA. However, TP was found to cause no changes in the DPA content of spores. Pressure is known to release DPA from spores there by sensitizing them to heat (*16*, *17*, *27*, *29*). The occurrence of changes in DPA content during PATP and nonoccurrence of similar changes in DPA content during TP suggests that PATP may sensitize spores by releasing DPA, followed by inactivation. Overall, the value of discriminating powers in PATP-treated spore samples is significantly higher than the discriminating power values in TP-treated spore samples, indicating greater extent of change during PATP than TP. PATP caused more number of changes (indicated by more number of peaks) in spores than TP. This suggests that combined pressure and temperature treatment has a multipronged inactivation mechanism that is more effective than temperature treatment alone.

Rapid Screening of Spores Resistant to Pressure-Assisted Thermal Processing. The resistances of the five strains investigated in this research to PATP were found to be in the following order: *B. amyloliquefaciens* Fad 82 > *B. amyloliquefaciens* Fad 11/2 > *B. amyloliquefaciens* ATCC 49764 > *B. sphaericus* NZ 14 > *C. tyrobutyricum* ATCC 25755 (**Table 1**). *Bacillus amyloliquefaciens* Fad 82 has been suggested as possible surrogate organism for studying the effectiveness of combined pressure and temperature processing (*5*, *7*). By comparing the biochemical composition of the PATP-resistant *B. amyloliquefaciens* Fad 82 with other organisms, the infrared bands and associated compounds that contribute to PATP-resistance could be inferred. **Figure 7** highlights the overall compositional difference between *B. amyloliquefaciens* Fad 82 and the other four strains investigated in this research. Major differences between *B. amyloliquefaciens* Fad 82 (most resistant) and *C. tyrobutyricum* ATCC 25755 (least resistant) were in DPA and Ca-DPA (1378, 1695, 1568, 1281, and 1440 cm^{-1}) and secondary proteins (1626 and 1655 cm^{-1}) (**Figure 7**, line **a**). The discriminating power for the difference between *C. tyrobutyricum* and *B. amyloliquefaciens* Fad 82 was the largest, indicating that these two strains are the most different in terms of composition. *Bacillus sphaericus* was also found be different in similar regions (**Figure 7**, line **b**). However, the discriminating power was lower than *C. tyrobutyricum*,implying that *B. sphaericus* is more similar in composition to *B. amyloliquefaciens* Fad 82 than *C. tyrobutyricum*. *Bacillus amyloliquefaciens* ATCC 49764 was only slightly different from *B. amyloliquefaciens* Fad 82 (**Figure 7**, line **c**). The difference was mainly in Ca-DPA content (1378 cm^{-1}). *Bacillus amyloliquefaciens* Fad 11/2 was found to be the most similar to *B. amyloliquefaciens* Fad 82 (**Figure 7**, line **d**) with relatively very small difference in Ca-DPA content.

Interestingly, the difference in the Ca-DPA content between *B. amyloliquefaciens* Fad 82 and other strains could be correlated to the PATP-resistance. By using *B. amyloliquefaciens* Fad 82 as reference for comparison, the peak height due to Ca-DPA (1378 cm^{-1}) reduced with increasing PATP-resistance. The least resistant strain, *C. tyrobutyricum*, had the largest difference in Ca-DPA content from *B. amyloliquefaciens* Fad 82. *Bacillus amyloliquefaciens* Fad 11/2, which has slightly lower resistance to PATP than *B. amyloliquefaciens* Fad 82, had the smallest difference in Ca-DPA content. Peaks of secondary proteins (1626 and 1655 cm^{-1}) also showed possible correlations with PATP-resistance. As evident in **Figure 7**, the peak height at 1626 and 1655 cm^{-1} reduced with increasing PATP-resistance. These data suggest that identification of unique infrared spectral signatures (possibly related to Ca-DPA content) could provide information regarding the PATP-resistance of spores.

The resistance of bacterial spores to certain processing/sterilization method is currently determined by traditional plating methods that are time consuming and expensive in the long run. A rapid screening method based on FT-IR spectroscopy by monitoring few selected compositional parameters can be a valuable tool to industry and research institutions. PATP-resistance could be influenced by many other factors other than Ca-DPA, including stability of the cortex and membrane. The proposed screening method needs further investigation with many different species and strains of spores. Additionally, whether or not this technique can be used to screen for TP-resistant spores also needs to be investigated. In this research, TP was not found to cause major changes in DPA content. Hence, spectral peaks other than DPA compounds may have to be monitored to draw inferences about TP-resistance. Nevertheless, the proposed rapid screening method shows promise and provides opportunities for further research.

To conclude, this study shows that a rapid technique based on FT-IR spectroscopy combined with multivariate classification algorithms could be used to discriminate and identify bacterial spores to the strain level based on difference in chemical composition, mainly secondary proteins and DPA. FT-IR spectroscopy also provided unique information for understanding the biochemical and structural changes in spores during inactivation. Rapid changes were found to occur in secondary structure of proteins and DPA content during initial stages of PATP. DPA release was evident during PATP treatment. We observed a correlation between Ca-DPA levels and the spore's resistant to PATP, which could be used for screening PATP-resistant bacterial spores. Although this study provided some insights into the biochemical changes occurring in spore during inactivation by PATP, the exact role of many components including DPA and their processing condition-dependent role in inactivation of spores is yet to be understood clearly. Nevertheless, FT-IR spectroscopy shows promise as a simple and rapid tool for investigating the mechanism of spore inactivation during processing.

LITERATURE CITED

(1) San Martin, M. F.; Barbosa-Canovas, G. V.; Swanson, B. G. Food processing by high hydrostatic pressure. *Crit. Rev. Food Sci. Nutr.* **2002**, *42*, 627–645.

(2) Mallidis, C. G.; Drizou, D. Effect of simultaneous application of heat and pressure on the survival of bacterial spores. *J. Appl. Bacteriol.* **1991**, *71*, 285–288.

(3) Matser, A. M.; Krebbers, B.; van den Berg, R. W.; Bartels, P. V. Advantages of high pressure sterilization on quality of food products. *Trends Food Sci. Technol.* **2004**, *15*, 79–85.

(4) Rajan, S.; Ahn, J.; Balasubramaniam, V. M.; Yousef, A. E. Combined pressure-thermal inactivation kinetics of *Bacillus amyloliquefaciens* spores in egg patty mine. *J. Food Prot.* **2006**, *69*, 853–860.

(5) Ahn, J.; Balasubramaniam, V. M.; Yousef, A. E. Inactivation kinetics of selected aerobic and anaerobic bacterial spores by pressure-assisted thermal processing. *Int. J. Food Microbiol.* **2007**, *113*, 321–329.

(6) Margosch, D.; Ehrmann, M. A.; Buckow, R.; Heinz, V.; Vogel, R. F.; Ganzle, M. G. Pressure inactivation of *Bacillus* endospores. *Appl. Environ. Microbiol.* **2006**, *72*, 3476–3481.

(7) Margosch, D.; Ehrmann, M. A.; Ganzle, M. G.; Vogel, R. F. Comparison of pressure and heat resistance of *Clostridium botulinum* and other endospores in mashed carrots. *J. Food Prot.* **2004**, *67*, 2530–2537.

(8) Okazaki, T.; Kakugawa, K.; Yoneda, T.; Suzuki, K. Inactivation behavior of heat-resistant bacterial spores by thermal treatments combined with high hydrostatic pressure. *Food Sci. Technol. Res.* **2000**, *6*, 204–207.

(9) Miglioli, L,; Gola, S.; Maggi, A.; Rovere, P.; Carpi, G.; Scaramuzza, N.; Dallaglio, G. Microbiological stabilization of low acid food using a combined high pressure-temperature process. In *High Pressure Research in the Bioscience and Biotechnology*; Hermans, K., Ed.; Leuven University Press: Belgium, 1997; pp 277–280.

(10) Setlow, P. Spores of *Bacillus subtilis*: their resistance to and killing by radiation, heat and chemicals. *J. Appl. Microbiol* **2006**, *101*, 514–525.

(11) Gould, G. W. History of science—spores. *J. Appl. Microbiol.* **2006**, *101*, 507–513.

(12) Setlow, P. Spore germination. *Curr. Opin. Microbiol.* **2003**, *6*, 550–556.

(13) Russell, A. D. Lethal effects of heat on bacterial physiology and structure. *Sci. Prog.* **2003**, *86*, 115–137.

(14) Gerhardt, P.; Marquis, R. E. Spore thermoresistance mechanisms. In *Regulation of Prokaryotic Development*; Smith, I., Slepecky, R. A., Setlow, R., Ed.; American Society of Microbiology: Washington, DC, 1989; pp 43–63.

(15) Paidhungat, M.; Setlow, B.; Driks, A.; Setlow, P. Characterization of spores of *Bacillus subtilis* which lack dipicolinic acid. *J. Bacteriol.* **2000**, *182*, 5505–5512.

(16) Paidhungat, M.; Setlow, B.; Daniels, B.; Hoover, D.; Papafragkou, E.; Setlow, P. Mechanisms of induction of germination of *Bacillus subtilis* spores by high pressure. *Appl. Environ. Microbiol* **2002**, *68*, 3172–3175.

(17) Wuytack, E. Y.; Boven, S.; Michiels, C. W. Comparative study of pressure-induced germination of spores at low and high pressures. *Appl. Environ. Microbiol.* **1998**, *64*, 3220–3224.

(18) Mariey, L.; Signolle, J. P.; Travert, A. J. Discrimination, classification, identification of microorganisms using FTIR spectroscopy and chemometrics. *Vib. Spectrosc.* **2001**, *26*, 151–159.

(19) Subramanian, A. S.; Ahn, J.; Balasubramaniam, V. M.; Rodriguez-Saona, L. Determination of spore inactivation during thermal and pressure-assisted thermal processing using FT-IR spectroscopy. *J. Agric. Food Chem.* **2006**, *54*, 10300–10306.

(20) Perkins, D. L.; Lovell, C. R.; Bronk, B. V.; Setlow, B.; Setlow, P. Fourier transform infrared reflectance microspectroscopy study of *Bacillus subtilis* engineered without dipicolinic acid: The contribution of calcium dipicolinate to the mid-infrared absorbance of *Bacillus subtilis* endospores. *Appl. Spectrosc.* **2005**, *59*, 893–896.

(21) Perkins, D. L.; Lovell, C. R.; Bronk, B. V.; Setlow, b.; Setlow, P.; Myrick, M. L. Effects of autoclaving on bacterial endospores studied by Fourier transform infrared microspectroscopy. *Appl. Spectrosc* **2004**, *58*, 749–753.

(22) Thompson, S. E.; Foster, N. S.; Johnson, T. J.; Valentine, N. B.; Amonette, J. E. Identification of bacterial spores using statistical analysis of Fourier transform infrared photoacoustic spectroscopy data. *Appl. Spectrosc.* **2003**, *57*, 893–899.

(23) Goodacre, R.; Shann, B.; Gilbert, R. J.; Timmins, E. M.; McGovern, A. C.; Alsberg, B. K.; Kell, D. B.; Logan, N. A. Detection of the dipicolinic acid biomarker in *Bacillus* spores using curie-point pyrolysis mass spectrometry and Fourier transform infrared spectroscopy. *Anal. Chem.* **2000**, *72*, 119–127.

(24) Cheung, H. Y.; Cui, J.; Sun, S. Real-time monitoring of *Bacillus subtilis* endospore components by attenuated total reflection Fourier-transform infrared spectroscopy during germination. *Microbiology* **1999**, *145*, 1043–1048.

(25) Kansiz, M.; Heraud, P.; Wood, B.; Burden, F.; Beardall, J.; McNaughton, D. Fourier transform infrared microspectroscopy and chemometrics as a tool for the discrimination of cyanobacterial strains. *Phytochemistry* **1999**, *52*, 407–417.

(26) Mark, H. Data analysis: Multilinear regression and principal component analysis. In *Handbook of Near-Infrared Analysis*; Burns, D. A., Ciurczak, E. W., Ed.; Taylor and Francis: New York, 2001; pp 129–184.

(27) Black, E. P.; Koziol-Dube, K.; Guan, D.; Wei, J.; Setlow, B.; Cortezzo, D. E.; Hoover, D. G.; Setlow, P. Factors influencing the germination of *Bacillus subtilis* spores via the activation of nutrient receptors by high pressure. *Appl. Environ. Microbiol.* **2005**, *71*, 5879–5887.

(28) Paidhungat, M.; Setlow, P. Spore germination and outgrowth. In *Bacillus subtilis and its relatives: From Genes to Cells*;Hoch, J. A., Losick, R., Sonenshein, A. L., Ed.; American Society of Microbiology: Washington, DC, 2001; pp 537–548.

(29) Wuytack, E. Y.; Soons, J.; Poschert, F.; Michiels, C. W. Comparative study of pressure- and nutrient-induced germination of *Bacillus subtilis* spores. *Appl. Environ. Microbiol.* **2000**, *66*, 257–261.

Received for review March 20, 2007. Revised manuscript received August 28, 2007. Accepted August 29, 2007. We thank the National Science Foundation I/UCRC and Center for Advanced Processing and Packaging Studies for funding this project.

JF0708241